Proceedings of International Conference on Heat Exchanger Fouling and Cleaning - 2015 (Peer-reviewed)
June 07 - 12, 2015, Enfield (Dublin), Ireland
Editors: M.R. Malayeri, H. Müller-Steinhagen and A.P. Watkinson
Published online
www.heatexchanger-fouling.com

INVESTIGATION BY RAMAN SPECTROSCOPY OF THE CONFORMATIONAL STRUCTURE OF WHEY PROTEINS CONSTITUTING FOULING DEPOSITS DURING THE PROCESSING IN A PLATE HEAT EXCHANGER - ROLE OF THE BETA-LACTOGLOBULIN MOLTEN GLOBULE

P. Blanpain-Avet [1], A. Hédoux [2], L. Paccou [2], Y. Guinet [2], T. Six [1], M. Khaldi [1] and G. Delaplace [1]

[1] INRA, UR638 - PIHM (Processus aux Interfaces et Hygiène des Matériaux), UMET (Unité Matériaux Et Transformations) UMR CNRS 8207 , 369, rue Jules Guesde, BP 20039, F-59651 Villeneuve d'Ascq Cedex (France).
E-mail (Corresponding author): blanpain-avet@lille.inra.fr

[2] UMET (Unité Matériaux Et Transformations), MMT (Matériaux Moléculaires et Thérapeutiques), UMR CNRS 8207, Université de Lille 1, F-59650 Villeneuve d'Ascq (France)

ABSTRACT

During the pasteurization process in the dairy industry, fouling of plate heat exchangers (PHEs) is a severe problem notably because the relationship between the build-up of protein fouling deposits and the chemical reactions taking place into the fouling solution has not yet been fully elucidated. The purpose of the present work was to show that the molten globule state of beta-lactoglobulin (β-lg) plays a key role in the build-up of whey protein deposits. Whey protein fouling deposits generated on the hot wall downstream a PHE were analyzed by micro Raman spectroscopy (MRS) carried out in the 800-1800 cm^{-1} range. Deposits were formed using a model β-lg fouling solution which was made using a whey protein isolate powder (89 wt % in β-lg) and a known amount of calcium. Thermal denaturation of the fouling solution was also analyzed by MRS as well as isolated β-lg aggregates. Specific Raman signatures of aggregates were identified, which were not detected in the Raman spectra of denatured (i.e., unfolded β-lg molecule) solutions. MRS analyses at different depths of the deposit reveal a loss of α-helix structures, as observed in denatured β-lg solutions, without the detection of aggregate signatures. Results suggest that the mass distribution of fouling in a PHE is primarily controlled by the distribution of the unfolded protein generated by the denaturation process.

INTRODUCTION

Fouling of heat exchangers in the dairy industry (mostly plate heat exchangers, PHEs) is still a serious issue. For a temperature below 110°C, the deposit is largely a "milk film" deposit or a type A (protein) fouling, consisting of 50-70 wt % proteins, 30-40 wt % minerals and 4-8 wt % fat (Bansal and Chen, 2006). It has been largely shown in the literature that β-lg plays a predominant role in milk fouling deposits.

The scientific community has examined the β-lg conformational structure and its link with temperature for several decades. At room temperature and at pH 7, the secondary structure of native β-lg is mainly composed of β-sheets (54 %) and α-helices (17 %) (Seo et al., 2010). Literature data show that an increase in temperature initiates a heat denaturation process which leads to different β-lg protein conformations in addition to the native one, i.e., unfolded and aggregated state (see Tolkach and Kulozik, 2007). Today it is well established that when heated in a neutral aqueous solution, globular molecules of β-lg unfold with a loss of their tertiary and secondary structure. Such unfolding of the protein exposes reactive sulphydryl (–SH) groups which are normally contained within the core of protein and permits the formation of disulphide bridges with different denatured proteins present in the solution (for example casein, α-lactalbumin), resulting in the formation of aggregates (Lalande et al., 1989).

Calorimetric and spectroscopic investigations of β-lg thermal denaturation, under different conditions of temperature, pH and protein concentration were carried out. Among them, one can mention those of Nonaka et al. (1993), Ikeda and Li-Chan (2004), Ngarize et al. (2004) and Seo et al. (2010). These studies conclude that a heat treatment induces changes in the β-lg secondary structure. There is notably a trend toward an increase in β-sheet structures at the expense of α-helices structures with a simultaneous decrease of turn structure when heating from 70 and 90°C. Using Raman scattering in the region of amide modes (800-1800 cm^{-1}), the mechanism of β-lg thermal denaturation in the 20-100°C temperature range could be described as a two-step process (Seo et al., 2010). The first step corresponds to the dissociation of dimers associated with the softening of the tertiary structure (observed between room temperature and 65°C). At the end of this step (around 65°C), the so-called ″molten globule state″ is obtained prior to conformational changes of the secondary structure taking place between 65 and 95°C (Seo et al., 2010). The detailed thermal behaviour of β-lg at pH > 6.8 and at temperatures up to 150°C has been recently described by the review paper of de Wit (2009).
Although the connection between the thermal stability and conformational changes of β-lg is well established, the role of the denaturated and aggregated species on the build-up of the fouling deposit onto a heat exchange surface is still unclear. Indeed, few studies take sides unreservedly whether β-lg fouling is controlled by β-lg aggregation rather than by denaturation. Trends reported in the literature are not really conclusive as regards which species is involved in protein

deposits, as underlined by Bansal and Chen (2006). Moreover, it is not obvious from the analysis of mechanistic models dealing with the prediction of fouling deposits in the literature to guess which species (unfolded or aggregated) shapes the fouling deposit. For example, Mahdi et al. (2009) and Jun and Puri (2007) assumed that only the aggregated protein is deposited on the wall, which is not functional for the model of de Jong et al. (1992, 1993) for which it is hypothesized that the main mechanism in fouling process is a reaction-controlled adsorption of unfolded β-lg. More detailed information regarding the involvement of protein denaturation and protein aggregation as governing reaction in fouling mechanisms is given in the review paper of Bansal and Chen (2006) to which the reader can refer.

More information on the conformational structure of the whey protein molecules (especially β-lg) which are present within a dairy protein deposit is required in order to elucidate the fouling mechanisms of PHEs. The molecular structure and conformation changes of proteins can be analyzed by Raman spectroscopy (RS) which is a technique capable of providing information with respect to peptide backbone conformation as well as environment of certain side chains (Nonaka et al., 1993 ; Li-Chan, 1996 ; Chi et al. 1998; Jung et al., 2000; Ngarize et al., 2004 ; Ikeda and Li-Chan, 2004). Chi et al. (1998) ascertained that the protein secondary structure can be determined from the analysis of the amide I, II and III bands and the $C_\alpha - H$ amide bending vibration. The amide (peptide) bond of proteins has several distinct vibrational modes, of which the amide I and III bands are the most useful for the study of secondary structure (Li-Chan, 1996). Jung et al. (2000) have demonstrated the potential of two-dimensional (2D) Raman correlation spectra and its complementarity with 2D infrared correlation spectra in the amide III region (1330-1200 cm^{-1}) to investigate the secondary structure of β-lg in a buffer solution at pH 6.6. Another advantage is that RS is a non destructive analytical technique capable of gaining data at high protein concentrations sufficient to cause gelation, i.e., as those encountered in a protein fouling deposit (Ikeda and Li-Chan, 2004).

Considering the dependence of the denaturation process of β-lg on pH, protein concentration, thermal history, and the controversial description of the denaturation mechanism (Seo et al., 2010), a denaturation curve (represented by the temperature dependence of the amide I band frequency in the 25-100°C temperature range) was carried out. For the denaturation curve, a 6 wt % whey protein isolate (WPI) solution with a calcium content of 264 $mg.l^{-1}$ dissolved in H_2O (pH 6.8) was used in order to characterize the heat-induced denaturation process. Additionally, prior to the Raman analysis of deposits, the Raman fingerprint of native, unfolded and aggregated β-lg was collected for a comparison purpose with deposit spectra.

The main objective of this study was to determine, by means of MRS, the nature of β-lg (i.e., native, denatured and aggregated β-lg) at the *deposit - stainless steel* surface interface and within the thickness of the deposit. This was carried out from the identification of the Raman signatures obtained during investigations of the β-lg thermal denaturation and from the analysis of aggregates in the (800 - 1800) cm^{-1} spectral range. A 6 wt. % WPI (purity in β-lg ~ 89 wt. %) solution was selected as a model fouling solution for which the heat induced denaturation/aggregation process of β-lg has been previously determined via a kinetic model (Petit et al., 2011). Additional deposits were generated using a 0.5 wt. % WPI solution with a calcium content ranging from 97 to 160 mg/l in order to investigate a possible role of calcium ions. Raman spectra of deposits in the amide I and amide III bands region (800-1800 cm^{-1}) were collected to measure possible changes in the secondary structure of β-lg within the successive layers of the deposit.

MATERIALS AND METHODS

Materials

Experimental equipment

Fouling experiments were conducted using a pilot plant described and represented in detail by Blanpain-Avet et al. (2012). Briefly, the fouling rig was composed of three distinct zones: a pre-heating zone composed of a tubular joule effect heater, noted JEH (Actijoule, Actini, 30 kW), a heating zone composed of a PHE (VICARB, model V2, Alpha-Laval, France) and a holding zone which was made up of a stainless steel pipe of 35 millimetres internal diameter, including a detachable fouling test surface which was set aside for MRS analysis. PHE set-up consisted of 13 plates forming twelve passes of one channel for the two sides. The equivalent space between two consecutive plates was 2.5 millimetres and the total exchange surface was 0.22 m². The capacity of the fouling solution tank was 300 litres and its temperature was regulated at (40 ± 1)°C using a tubular JEH (Actijoule, Actini, 15 kW).

The fouling test surface was composed of three stainless steel rings (type 304) of 22.6 millimeters internal diameter, 19 millimeters length, which were assembled in series within a 35 millimeters diameter pipe. The second ring in the middle of the pipe consisted of two semi-cylindrical assembled parts that were used specifically for MRS analysis in confocal mode with the incident laser beam of the spectrometer hitting the upper surface of the deposit; both remaining rings were used for MRS analysis of a profile line along the deposit cross section; this allowed to perform a MRS analysis in confocal mode (axial resolution ≈ 10 µm) both within the deposit thickness and along the deposit cross section.

Raman spectra

RS was performed using a Renishaw microspectrometer equipped with a confocal Leica microscope. The 514.5 nm radiation of a coherent Ar-Kr laser or the 785 nm line of a Renishaw laser diode was used depending on the fluorescence contribution of the sample. Spectra were recorded by measuring in backscattering geometry using gratings of groove density 1800 and 1200 grooves/mm for the 514.5 nm and 785 nm incident radiation respectively, giving a resolution of 2 cm^{-1} in the 800-1800 cm^{-1} range (fingerprint region) for both incident radiations. Thermal denaturation of the fouling solution was studied using the 785

nm radiation, while the deposit and aggregates were analyzed using the 514.5 nm radiation. Aggregates were analyzed at different points with the 100X objective. The same objective was used for the analysis of deposits; z-scans were performed from the surface of the deposit toward the deposit - stainless steel interface, with a step of typically 10 µm through the deposit . For analyses along the deposit cross section, X-scans were performed from the deposit-stainless steel interface to the upper layer of the deposit with a step generally equal to 5-10 µm. The Raman intensity was integrated in a cylindrical volume of 2.5 µm (depth) × 0.8 μm^2 (spot size) for both the deposit and the aggregate samples inherent to the wavelength of the incident radiation and the microscope objective.

Fouling solution

The test surface was fouled using a reconstituted industrial WPI powder at a 6 wt.% concentration (pH 6.8) and at a 6.6 mM ionic calcium content (anhydrous $CaCl_2$, 96 % min, Prolabo, VWR, USA). Such an ionic calcium content was selected as the experimental program of this study was part of the research program GLOBULE (ANR-08-ALIA-08). Three additional deposits were generated using a WPI solution at a 0.5 wt. % concentration with an atom calcium content (considering a molecular weight of 40.08 gramme per mole) equal to 97, 120 and 160 mg/l in order to detect a possible effect of calcium ions on deposit structure. This concentration was slightly higher than the β-lg concentration in milk, which varies between 0.3 and 0.4 wt. % (Bansal and Chen, 2006; Delplace et al., 1997). WPI powder composition was : 89 wt. % β-lg (in weight percent on a dry basis), α-lactalbumin (α-la) < 0.01 wt.% (β-lg and α-la were measured using RP-HPLC according to a methodology described by Petit et al., 2011), 0.1 wt % fat, 1.9 wt % ash, moisture 4.1 wt %. The experimental procedure of preparation of the fouling solution was the following : 15 kg of WPI powder was poured into 250 litres of deionised water maintained at 40°C in the launching tank and dissolving occurred during two hours by gently stirring the solution; then 187 g of anhydrous $CaCl_2$ was poured into the fouling solution before the fouling step launch. For the additional experiments using a 0.5 wt. % WPI solution, 1.25 kg of WPI powder was used instead of the 15 kg of WPI powder above using the same experimental dissolving procedure; then the appropriate amount of anhydrous $CaCl_2$ was poured into the fouling solution before the fouling step launch.

Methods

Fouling of the test surface by means of fouling-rinsing experiments

Each fouling and cleaning experiment consisted of five stages : initial stabilization of hydraulic and thermal parameters using reverse osmosis (RO) water circulation, fouling (crossflow velocity v of 0.1 m/s corresponding to a flow rate Q = 150 $l.h^{-1}$, turbulent flow regime, Re ≈ 6.8 x 10^3), first RO water rinse, NaOH-HNO_3 cleaning procedure and a final RO water rinse. The Reynolds number in the fouling test surface was computed based on physical properties of water, by assuming that the presence of a 6 wt. % WPI in water does not modify them significantly; Reynolds number was defined by : $Re = \rho.v.D/\mu$. During fouling, the tubular JEH was used for pre-heating the fouling solution to 60°C. PHE was used to heat the fouling solution above the denaturation temperature (from 60 to 85°C) in a counter-current mode. Hot water was used at the heating medium. In order to keep the feed composition constant, the fouling solution was not re-circulated once it was heated through the tubular JEH and PHE. During experiments, the inlet temperature of hot water was adjusted to ensure a constant outlet fouling solution temperature in the holding zone (wall temperature close to T_w = 85°C) as well as a constant profile of product temperature along the PHE as a function of time. In the beginning, the PHE was brought to thermal equilibrium and to the desired process temperature (i.e., T_w = 85°C) using RO water. The feed was then switched from RO water to the fouling solution and the fouling stage was continuated for about 1.7 hour. After the fouling experiment, fouling solution was replaced by RO water at room temperature to bring the temperature of the PHE and protein deposit to ambient temperature. Experimentally, following the first rinse, the test fouling surface was dismantled and carefully removed from the holding zone, then stored at room temperature for 24 hours at the most before the MRS analysis. In Fig. 1 are presented some representative photographs of the fouling layer deposited on semi-cylindrical assembled parts within the fouling test surface, showing a white, soft β-lg deposit.

Analysis of the β-lg thermal denaturation process and of aggregates by Raman spectroscopy

At laboratory scale for the MRS analysis of the thermal denaturation process, the experimental procedure for the preparation of the β-lg solution in H_2O was described in detail by Blanpain-Avet et al. (2012). Briefly, it consisted in dissolving the protein containing mixtures (at a 6 wt. % β-lg concentration) in an Eppendorf tube of 1.5 ml volume at about 25°C. Protein mixtures were then loaded in cylindrical glass cells hermetically closed and located in a THMS 600 Linkam temperature device. MRS measurements were carried out in the 20-90°C temperature range on samples at pH 6.8 in H_2O, by step of 5 degrees between 20 and 55 °C and by step of 2.5 degrees above 55 °C. The acquisition time for each spectrum was fifteen minutes. A 50X long-working distance objective was used leading to the analysis of 20 μm^3 of solution with the 785 nm incident radiation. With this thermal history, no evidence of aggregates could be detected optically using this objective. Additional reference spectra were recorded using a 10 wt. % β-lg solution for which β-lg was purchased from Sigma-Aldrich (Sigma-Aldrich Chemie s.a.r.l., France) as lyophilized powder (purity minimum 90 %).

Aggregates were formed by heating the fouling solution for one hour at 90°C in a stirred beaker. They were deposited by filtration under vacuum on a flat 0.2 µm polyethersulphone membrane prior to the MRS analysis at room temperature.

A 100X objective was used to analyze aggregates, resulting in the analysis of a volume of 2μm^3 with the 514.5 nm incident radiation.

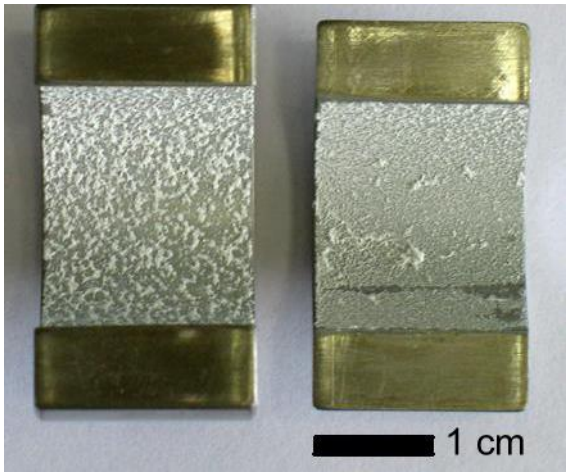

Fig. 1. Pictures of fouled test surfaces (semi-cylindrical assembled parts used for MRS analysis in confocal mode along the z axis) for a calcium content of 264 mg/l. Experimental conditions:T_w = 85°C, Q = 150 l/h.

A fluorescence contribution to the spectra appeared systematically in the background signal; its magnitude was approximated by a second order polynomial using a fitting procedure and then subtracted from the spectra. Assignment of the major bands of β-lg in the spectra to vibrational motions of various side chains or peptide backbone was based on comparison with Raman spectra of proteins reported or summarized in the literature (Chi et al., 1998; Ikeda and Li-Chan, 2004; Jung et al., 2000; Li-Chan, 1996; Ngarize et al., 2004; Nonaka et al., 1993; Seo et al., 2010; Ivleva et al. 2009).

Statistical analysis and processing of Raman spectra data

Statistical analyses were performed using Sigmastat 3.1 and Sigmaplot 10 software (Systat Software, Inc., Point Richmond, CA). The level of significance was $p<0.05$. Raman spectra were analyzed and deconvoluted using a nonlinear least-squares curve-fitting subroutine in Peakfit 4.12 software (Seasolve Software, Framingham, MA).

RESULTS AND DISCUSSION

Analysis using RS of the β-lg thermal denaturation in the fouling solution

Investigation of the amide modes in the (800-1800) cm^{-1} region. Assignment of major bands of β-lg

At room temperature and at the temperature of the holding zone in fouling runs (85°C), Raman spectra of the fouling solution (6 wt % β-lg in H_2O plus 264 mg.l^{-1} calcium, pH 6.8) in the (800-1800) cm^{-1} region are plotted in Fig. 2 for the assignment of Raman bands. Spectra were baselined and area normalized for a clear presentation of the bands. It is well accepted that the secondary protein structure can be analyzed in the amide I and amide III regions between 1550 and 1750 cm^{-1} and 1200-1350 cm^{-1}, respectively (Jung et al., 2000). The frequency position of these bands depends strongly on the protein state, the environment and the intermolecular interactions.

As shown in Fig. 2, the most intense band of the spectrum, located around 1650 cm^{-1}, is the amide I band (labelled (1) in Fig. 2). This band arises mainly from the C=O stretching vibration with minor contributions of the C–N stretching vibration, and the N–H in-plane bend (Seo et al., 2010). The band shape of the amide I mode can be considered as overlapping components corresponding to α-helices, β-sheets, turns and random structures. The weak intense band around 1550 cm^{-1} is the amide II band (labelled (2) in Fig. 2). It mainly corresponds to a mixture of N-H in-plane bend and C-N stretch. Both amide I and II regions are widely used for secondary structure analysis. However, taking into account its weak intensity in the Raman spectra of the β-lg solutions, band (2) will not be used to analyze the β-lg thermal denaturation. The vibrational composition of the amide III mode is complex, since NH bend contributes to several modes in the 1200-1400 cm^{-1} region. However, the range of vibrational frequencies observed for various secondary structures is greater than that for amide I and amide II. The Raman band located around 1240 cm^{-1} (3b) was assigned to β-sheet structure (Seo et al., 2010). These bands are observed well separated from the amide III mode corresponding to α-helix structures, located around 1320 cm^{-1} (3a) and from other bands at 940 and 960 cm^{-1} (labelled (4) in Fig. 2) also associated with α-helical conformation (Seo et al., 2010). The intensity of the band around 940 cm^{-1} (C–C–N stretching, α-helix) was considered to be proportional to the α-helix content (Ikeda, 2003, Ikeda and Li-Chan 2004). The C_α–H symmetric bending band located at about 1395 cm^{-1} (labelled (5) in Fig. 2) was found to have an intensity that decreased as the protein α-helical content increased (Chi et al., 1998).

Analysis of Raman spectra. Investigation of the amide modes in the (800-1800) cm^{-1} region

Thermal denaturation monitored by the amide I band for β-lg dissolved in H_2O

It has been shown that the frequency position of the intensity maximum of amide I band can be used to monitor conformational changes (Hédoux et al., 2006a, 2006b, 2009; Ionov et al., 2006; Seo et al., 2010). Fit of the amide I band region (1500-1800 cm^{-1}) was performed using a three-component (Gaussian) band fitting. The temperature dependence of the amide I band frequency ($\nu_{amide\ I}$) is represented in Fig. 3a for a 6 wt. % β-lg solution dissolved in H_2O. Upon heating, a frequency upshift of the intensity maximum is observed corresponding to conformational changes in the secondary structure previously described as a loss of α-helix structures and a formation of β-sheets (Seo et al., 2010). The temperature dependence of the amide I band frequency was fitted using a sigmoid curve :

$$\nu = \left[\left(\nu_N - \nu_D\right)/\left(1+\exp\left(\left(T - T_m\right)/\Delta T\right)\right)\right] + \nu_D \quad (1)$$

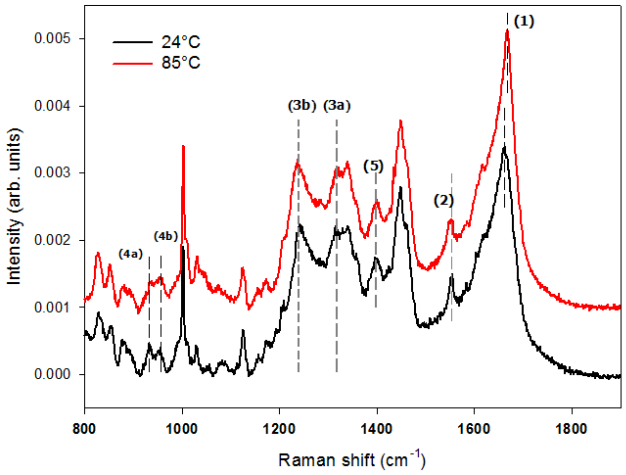

Fig. 2. Raman spectrum of the fouling solution at 25 and 85°C in the 800-1800 cm^{-1} region. The Raman bands represented by a vertical dashed line and labelled from (1) to (5) correspond to : (1) : amide I band (~1650 cm^{-1}), (2) : amide II band (~1550 cm^{-1}), (3a) amide III (α-helix, ~1320 cm^{-1}) and (3b) amide III (β-sheet, ~1240 cm^{-1}), (4a) 940 cm^{-1} (α-helix) and (4b) 960 cm^{-1} (α-helix), (5) C_α-H bending (~1395 cm^{-1}).

where T_m is the transition midpoint temperature, 2 x ΔT corresponds to the temperature domain of the transition, and ν_N and ν_D are the frequencies of the amide band in the native and denatured (totally unfolded) states, respectively. A least-square fit of experimental data is plotted in Fig. 3a for the β-lg solution, leading to T_m = (65.7 ± 1) °C.

Raman fingerprint of β-lg aggregates

The spectrum of aggregates is compared to that of the dry WPI powder in the 800 - 1800 cm^{-1} region and is plotted in Figures 4a and 4b. This comparison reveals Raman signatures corresponding to structural changes (Figs 4a and 4b) which are distinct from those observed in the denatured state of the fouling solution. They are localized by arrows in Figs 4a, 4b. An additional Raman band is observed near 1738 cm^{-1} ((1738.1 ± 0.8) cm^{-1}) together with a shift of the amide I band towards the high frequencies (average increase of (3.9 ± 0.1) cm^{-1} compared to native β-lg, with a statistically significant difference: p_{value}<0.001 as calculated using a one-way analysis of variance).
Spectrum differences in the amide I region between the native and denatured states of the fouling solution and between aggregates and dry (native) β-lg, are plotted in Figure 5. A common peak is observed around 1670 cm^{-1} for both spectrum differences, interpreted as an increase of β-sheet content. However, for aggregates this peak is sharp because of significant negative intensities with maxima around 1655 and 1690 cm^{-1}. Negative intensities above 1675 cm^{-1} can be interpreted as reflecting the increase of β-turns detected around 1680 cm^{-1} by IR spectroscopy (Czarnik-Matusewicz et al., 2000).

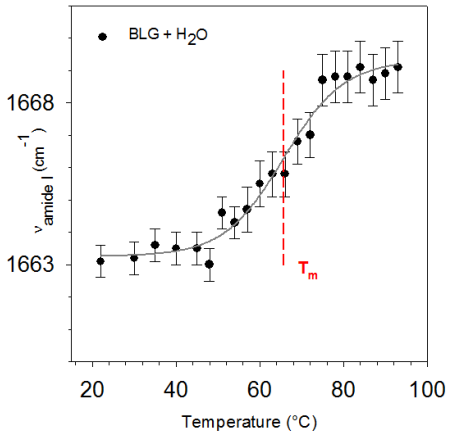

Fig. 3a. Temperature dependence of the amide I band frequency (component plotted in red dashed line, see Fig. 3b) for a 6 wt % β-lg solution dissolved in H_2O. T_m = (65.7 ± 1.3)°C is represented as a red dotted vertical line, indicating the midpoint of the unfolding transition determined by the fitting procedure and the amide I band frequency. The red solid line corresponds to the fitting procedure made using Eq. (1) and that is described in the text. Error bars correspond to the standard error on the $\nu_{amide\ I}$ value.

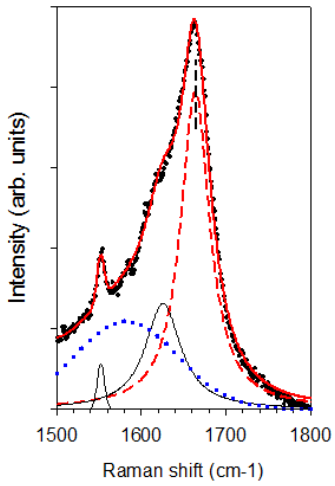

Fig. 3b. Fitting procedure of the spectrum in the amide I region. Four bands are necessary to obtain a good agreement between experimental data (crosshair) and the fitting curve (red solid line); three bands correspond to the components representative of the molecular conformation of the protein, while the dotted line corresponds to the contribution of the solvent (bending mode of H_2O). The red dashed line is the component which undergoes a frequency shift upon heating and is used for monitoring thermal denaturation.

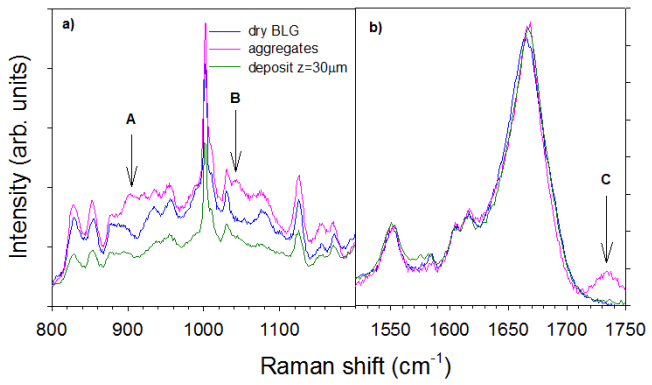

Fig. 4. Raman spectra in the 800-1200 cm^{-1} region (a) and in the amide I (1500-1750 cm^{-1}) region (b) for β-lg aggregates, dry β-lg powder and a deposit.

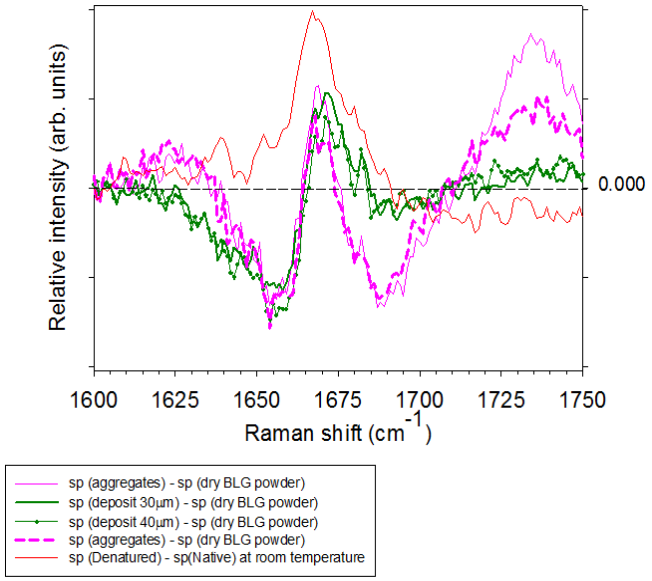

Fig. 5. Spectrum differences between β-lg aggregates and dry β-lg powder, between deposit and dry β-lg powder and between denatured β-lg (solution at 90°C) and native β-lg at room temperature. The term "sp" in the panelled-in caption means spectrum.

Evaluation of the molecular structure of β-lg within the fouling layer

The difference between the spectra of dry β-lg powder and the deposit is also plotted in Fig. 5. As regards spectrum differences between the deposit and dry (native) β-lg powder, the inspection of Figures 4a, 4b and Fig. 5 indicates : i) no noticeable peak close to the characteristic Raman band of β-lg aggregates near 1730 cm^{-1} (see the arrow labelled C, Fig. 4b), ii) the spectrum differences in the amide I region reveal Raman features distinct from aggregates above 1675 cm^{-1}, indicating that the secondary structure in the deposit is different from that in aggregates, that is, the increase of β-turn structures is only observed in aggregates. iii) Raman signatures of aggregates between 800 and 1200 cm^{-1} are not detected in the deposit (see the arrows labelled A, B in Fig 4a). The average frequency shift of the amide I band ranges from (1667.1 ± 0.4) cm^{-1} to (1667.6 ± 0.7) cm^{-1} within the deposit thickness for the various fouling runs compared to (1665.4 - 1665.6 ± 0.1) cm^{-1} for the dry WPI powder ; as a result, no significant difference of the $\nu_{amide\ I}$ values between deposits and the dry WPI powder (native β-lg) has been observed with $p > 0.05$ as calculated by ANOVA. These results suggest that aggregates are not the cause of β-lg deposits, since their Raman signatures were not detected into the deposit. This is in line with the conclusion drawn by Grijspeerdt et al. (2004) who stated, in their fouling model developed for ultra high temperature milk heat exchangers subjected to fouling, that aggregated β-lg was considered to play no significant role in the fouling process.

The content of calcium has been found not to have a significant effect on $\nu_{amide\ I}$ ($p=0.87$) and thus calcium ions (in the range (97 - 264) mg/l) have no impact on the β-lg molecular conformation within deposits.

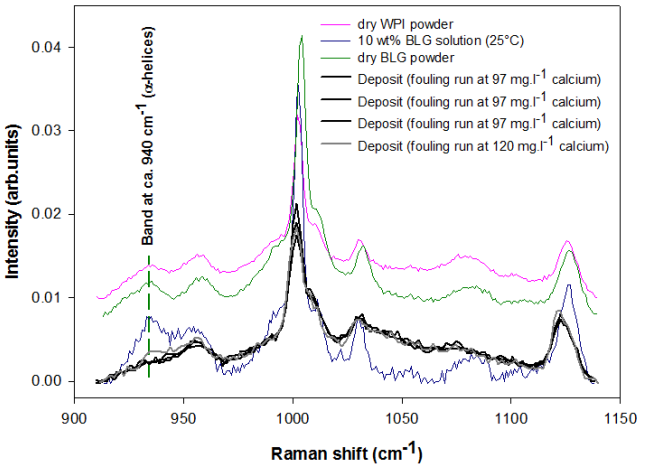

Fig. 6. Spectra in the amide III region (911 - 1140 cm^{-1}) of various deposits as compared with reference spectra of native β-lg (dry WPI powder, dry β-lg powder and a 10 wt.% β-lg in H_2O solution at 25°C).

Additional information on the secondary structure of β-lg in deposits could be further shown from the inspection of the band around 940 cm^{-1}, which is associated with the α-helical conformation (Ikeda, 2003a, 2003b; Ikeda and Li-Chan, 2004; Ngarize et al., 2004; Nonaka et al., 1993). According to Ikeda (2003a, 2003b), the normalized intensity of the band around 940 cm^{-1} is considered to be proportional to the α-helix content. We have thus compared spectra of native β-lg (i.e., β-lg at 25°C and the dry WPI powder) with those of various deposits at different calcium contents in the 0.5 wt % β-lg fouling solution, as presented in Fig. 6. In Fig. 6, spectra were normalized in the (911-1140) cm^{-1} range after subtraction of the baseline. The intensity of the band at ca. 940 cm^{-1} assigned to α-helices is observed to decrease for the deposits compared to the spectrum of native β-lg, which

supports a lower α-helix content of β-lg within deposits compared to native β-lg.

CONCLUSIONS

Micro-Raman spectroscopy was used to determine the molecular conformation of β-lg at the *deposit - stainless steel surface* interface from the knowledge of the Raman signatures of β-lg solutions. Raman signatures were recorded upon heating toward the thermal unfolded state and in aggregates, in the 800 - 1800 cm^{-1} frequency range. Deposits were generated by means of a fouling-rinsing sequence performed at pilot scale using a WPI solution at a 6 wt. % concentration with a calcium content fixed at 264 mg/l for which the heat-induced denaturation/aggregation process of β-lg has been previously determined via a kinetic model (Petit et al., 2011); additional deposits were generated using a 0.5 wt. % WPI solution with a calcium content ranging from 97 to 160 $mg.l^{-1}$.

It was found that the molecular conformation of the protein at the *stainless steel-deposit* interface was characterized by a frequency shift of the amide I band and by an intensity decrease of the 940 cm^{-1} band, consistent with a loss of α-helix structures. No evidence of aggregates was detected in deposits. These analyzes suggest that, in our range of operating conditions (T_w = 85°C, turbulent flow regime), the mass distribution of the fouling deposit in a PHE is solely controlled by the distribution of the unfolded protein generated by the denaturation process.

For the range of calcium content investigated, it has been shown that the presence of calcium ion did not affect significantly the molecular conformation of β-lg within the deposit. Further analysis of the variation of $\nu_{amide\ I}$ as a function of the deposit thickness in confocal mode as well as the intensity of the band around 940 cm^{-1} (which is associated with the α-helical conformation) revealed that: i) the α-helix content for β-lg within deposits is likely to be lower than that of native β-lg and ii) the loss of α-helix structures is enhanced at a high calcium content for β-lg molecules close to the *stainless steel - deposit* interface. The latter point needs to be confirmed by additional RS analyses on deposits.

This study by means of RS carried out at the *deposit - stainless steel surface* interface was shown to be able to elucidate the impact of the denaturation and aggregation reactions of β-lg on the fouling mechanism of a heat exchanger by milk proteins. Further research will focus on the effect of the wall temperature (T_w) on the conformational structure of β-lg at the *fluid-stainless steel surface* interface by varying T_w above and below a critical wall temperature (close to 80°C for the model fouling solution used, according to Petit et al., 2011) for which aggregates and the unfolded protein prevail, respectively. This will allow to elucidate if the governing reaction in fouling mechanisms is protein denaturation or protein aggregation.

ACKNOWLEDGEMENTS

This work was carried out within the framework of an ARCIR ("Actions de Recherche Concertées d'Initiative Régionale") program (European regional development fund 09 310 243 and 03 310 241), which joined non elucidated scientific issues of the Globule project (ANR-08-ALIA-08).

NOMENCLATURE

D Internal diameter of the pipe within the test fouling surface (=0.0226), m
Q Flow rate in the fouling stage, m^3/s
Re Reynolds number of the fouling solution during the fouling step within the test fouling surface (= 6.8 x 10^3), dimensionless
T Temperature, °C
T_m Transition midpoint temperature for the β-lg folding-unfolding transition, °C
T_w Wall temperature in the holding zone, °C
v Crossflow velocity within the test fouling surface, m/s
X Length of the deposit cross section related to the MRS analysis using a profile line, µm
z Deposit thickness related to the MRS analysis onto the deposit surface, µm

Symbols

ΔT 2 x ΔT corresponds to the temperature domain of the *folding-unfolding* transition, °C
$\nu_{amide\ I}$ Amide I band frequency, cm^{-1}
ν_D Frequency of the amide I band in the denatured (unfolded) state, cm^{-1}
ν_N Frequency of the amide I band in the native state, cm^{-1}
μ Dynamic viscosity of solution, kg/m s
ρ Specific mass of solution; kg/m^3

Abbreviations

ANOVA Analysis of variance
β-lg Beta-lactoglobulin (also noted BLG)
JEH Joule effect heater
MRS Raman micro-spectroscopy
PHE Plate heat exchanger
RO Reverse osmosis
RS Raman spectroscopy
WPI Whey protein isolate

REFERENCES

Bansal, B. and Chen, X.D., 2006, A critical review of milk fouling in heat exchangers, *Comprehensive Reviews in Food Science and Food Safety*, Vol. 5, pp. 27-33.

Blanpain-Avet, P., Hédoux, A., Guinet, Y., Paccou, L., Petit, J., Six, T., and Delaplace G., 2012, Analysis by Raman spectroscopy of the conformational structure of whey proteins constituting fouling deposits during the processing in a heat exchanger, *J. Food Eng*., Vol. 110, pp. 86-94.

Chi, Z., Chen, X.G., Holtz, J.S.W. and Asher, S.A., 1998, UV resonance Raman-selective amide vibrational enhancement: quantitative methodology for determining protein secondary structure, *Biochemistry*, Vol. 37 (9), pp. 2854-2864.

Czarnik-Matusewicz, B., Murayama, K., Wu, Y. and Ozaki, Y., 2000, Two-dimensional attenuated total reflection/infrared correlation spectroscopy of adsorption-induced and concentration-dependent spectral variations of β-lactoglobulin in aqueous solutions, *Journal of Physical Chemistry B*, Vol. 104, pp. 7803-7811.

Delplace, F., Leuliet, J.C. and Devieux, D., 1997, A reaction engineering approach to the analysis of fouling by whey proteins of a six-channels-per-pass plate heat exchanger, *J. Food Engineering*, Vol. 34, pp. 91-108.

De Jong, P., Bouman, S. and Van Der Linder, H.J, 1992, Fouling of heat treatment equipment in relation to denaturation of β-lactoglobulin. *Journal of the Society of Dairy Technology*, Vol. 45 (1), pp. 3-8.

De Jong, P., Waalewijn, R. and Van Der Linden, H.J., 1993, Validity of a kinetic fouling model for heat treatment of whole milk, *Le Lait*, Vol. 73(3), pp.293-302.

De Wit, J.N., 2009, Thermal behaviour of bovine β-lactoglobulin at temperatures up to 150°C. A review, *Trends in Food Science and Technology*, Vol. 20, pp. 27-34.

Grijspeerdt, K., Mortier, L., De Block, Jan, and Van Renterghem, R., 2004, Applications of modelling to optimise high temperature milk heat exchangers with respect to fouling. *Food Control*, Vol. 15, pp. 117-130.

Hédoux, A., Ionov, R., Willart, J.F., Lerbret, A., Affouard, F., Guinet, Y., Descamps, M., Prévost, D., Paccou, L. and Danède, F., 2006a, Evidence of a two-stage thermal denaturation process in lysozyme: A Raman scattering and differential scanning calorimetry investigation. *The Journal of Chemical Physics*, Vol. 124, p. 014703.

Hédoux, A., Willart, J.F., Ionov, R., Affouard, F., Guinet, Y., Paccou, L., Lerbret, A. and Descamps, M., 2006b, Analysis of sugar bioprotective mechanisms on the thermal denaturation of lysozyme from Raman scattering and differential scanning calorimetry investigations. *Journal of Physical Chemistry B*, Vol. 110, pp. 22886-22893.

Hédoux, A., Willart, J.F., Paccou, L., Guinet, Y., Affouard, F., Lerbret, A. and Descamps, M., 2009, Thermostabilization mechanism of bovine serum albumin by trehalose. *Journal of Physical Chemistry B*, Vol. 113, pp. 6119-6126.

Ikeda, S., 2003a, Heat-induced gelation of whey proteins observed by rheology, atomic force microscopy and Raman scattering spectroscopy, *Food Hydrocolloids*, Vol. 17, pp. 399-406.

Ikeda, S., 2003b, Atomic force microscopy and Raman scattering spectroscopy studies on heat-induced fibrous aggregates of β-lactoglobulin, *Spectroscopy*, Vol. 17, pp. 195-202.

Ikeda, S. and Li-Chan, E.C.Y., 2004, Raman spectroscopy of heat-induced fine-stranded and particulate β-lactoglobulin gels, *Food Hydrocolloids*, Vol. 18, pp. 489-498.

Ionov, R., Hédoux, A., Guinet, Y., Bordat, P., Lerbret, A., Affouard, F., Prevost, D. and Descamps, M., 2006, Sugar bioprotective effects on thermal denaturation of lysozyme: Insights from Raman scattering experiments and molecular dynamics simulation, *Journal of Non-Crystalline Solids*, Vol. 352, pp. 4430-4436.

Ivleva, N., Wagner, M., Horn, H., Niessner, R. and Haisch, C., 2009, Towards a nondestructive chemical characterization of biofilm matrix by Raman microscopy, *Analytical and Bioanalytical Chem.*, Vol. 393, pp. 197-206.

Jun, S. and Puri, V.M, 2007, Plate heat exchanger: thermal and fouling analysis, In Da-Wen-Sun (Ed.), *Computational fluid dynamics in food processing* (pp. 417-432). CRC Press, Taylor & Francis Group.

Jung, Y.M., Czarnik-Matusewicz, B. and Ozaki, Y., 2000, Two-dimensional infrared, two-dimensional Raman and two-dimensional infrared and Raman heterospectral correlation studies of secondary structure of β-lactoglobulin in buffer solutions, *Journal of Physical Chemistry B*, Vol. 104, pp. 7812-7817.

Lalande, M., René, F. and Tissier, J.P., 1989, Fouling and its control in heat exchangers in the dairy industry, *Biofouling*, Vol. 1, pp. 233-250.

Li-Chan, E.C.Y., 1996, The applications of Raman spectroscopy in food science, *Trends in Food Science and Technology*, Vol. 7, pp. 361-370.

Mahdi, Y., Mouheb, A. and Oufer, L., 2009, A dynamic model for milk fouling in a plate heat exchanger, *Applied Mathematical Modelling*, Vol. 33, pp. 648-662.

Ngarize, S., Herman, H., Adams, A. and Howell, N., 2004, Comparison of changes in the secondary structure of unheated, heated, and high pressure treated β-lactoglobulin and ovalbumin proteins using Fourier transform Raman spectroscopy and self-deconvolution, *Journal of Agricultural and Food Chemistry*, Vol. 52, pp. 6470-6477.

Nonaka, M., Li-Chan, E. and Nakai, S., 1993, Raman spectroscopic study of thermally induced gelation of whey proteins. *Journal of Agricultural and Food Chem*istry, Vol. 41, pp. 1176-1181.

Petit, J., Herbig, A.L., Moreau, A. and Delaplace, G., 2011, Influence of calcium on β-lactoglobulin denaturation kinetics: implications in unfolding and aggregation mechanisms, *J. Dairy Science*, Vol. 94 (12), pp. 5794-5810.

Seo, J. A., Hédoux, A., Guinet, Y., Paccou, L., Affouard, F., Lerbret, A. and Descamps, M., 2010, Thermal denaturation of beta-lactoglobulin and stabilization mechanism by trehalose analyzed from Raman spectroscopy investigations, *Journal of Physical Chemistry B*, Vol. 114 (19), pp. 6675-6684.

Tolkach, A. and Kulozik, U., 2007, Reaction kinetic pathway of reversible and irreversible thermal denaturation of β-lactoglobulin, *Le Lait*, Vol. 87, pp. 301-315.